Bioorganic & Medicinal Chemistry Letters xxx (2013) xxx–xxx

Contents lists available at SciVerse ScienceDirect

Bioorganic & Medicinal Chemistry Letters

journal homepage: www.elsevier.com/locate/bmcl

A hit to lead discovery of novel *N*-methylated imidazolo-, pyrrolo-, and pyrazolo-pyrimidines as potent and selective mTOR inhibitors

Wendy Lee [a,*], Daniel F. Ortwine [a,*], Philippe Bergeron [a], Kevin Lau [a], Lichuan Lin [c], Shiva Malek [b], Jim Nonomiya [b], Zhonghua Pei [a], Kirk D. Robarge [a], Stephen Schmidt [b], Steve Sideris [b], Joseph P. Lyssikatos [a]

[a] Department of Discovery Chemistry, Genentech, Inc., 1 DNA Way, South San Francisco, CA 94080, USA
[b] Department of Biochemical Pharmacology, Genentech, Inc., 1 DNA Way, South San Francisco, CA 94080, USA
[c] Drug Metabolism and Pharmacokinetics, Genentech, Inc., 1 DNA Way, South San Francisco, CA 94080, USA

ARTICLE INFO

Article history:
Received 20 May 2013
Revised 10 July 2013
Accepted 16 July 2013
Available online xxxx

Keywords:
Mammalian target of rapamycin
mTOR kinase inhibitors
PI3K/Akt/mTOR pathway
Structure based design
Oncology

ABSTRACT

A series of *N*-7-methyl-imidazolopyrimidine inhibitors of the mTOR kinase have been designed and prepared, based on the hypothesis that the *N*-7-methyl substituent on imidazolopyrimidine would impart selectivity for mTOR over the related PI3Kα and δ kinases. The corresponding *N*-Me substituted pyrrolo[3,2-*d*]pyrimidines and pyrazolo[4,3-*d*]pyrimidines also show potent mTOR inhibition with selectivity toward both PI3α and δ kinases. The most potent compound synthesized is pyrazolo[4,3-*d*]pyrimidine **21c**. Compound **21c** shows a K_i of 2 nM against mTOR inhibition, remarkable selectivity (>2900×) over PI3 kinases, and excellent potency in cell-based assays.

The mammalian target of rapamycin (mTOR) is a serine/threonine protein kinase of the phosphoinositide 3-kinase-related kinase (PIKK) family and a key point for inhibition downstream in the PI3K–Akt signaling pathway. mTOR plays a central role as a regulator of cell growth, proliferation, metabolism, and survival.[1] Inhibition of mTOR signaling can be used for treating solid tumors with mutations or deletion of the tumor suppressor phosphatase and tensin homolog (PTEN) gene.[2] The mTOR signaling pathway consists of two different multi-protein complexes: mTOR complex-1 (mTORC1) and mTOR complex-2 (mTORC2). mTORC1 is known for its critical role in protein synthesis and can phosphorylate two key regulators of protein translation, 4EBP and S6K. mTORC2 can phosphorylate Akt and functions as a key regulator of cell growth, metabolism, and survival. In certain cancer cells, Akt activity is upregulated and enhances cell survival due to a feedback loop between mTORC1 and Akt.[3] The natural product rapamycin, and semi-synthetic analogs thereof, selectively inhibit mTORC1 activity in an allosteric manner.[4] These so-called 'rapalogs' have beenused clinically to validate mTOR as a cancer target. Second generation mTOR inhibitors are small molecules that bind competitively and reversibly to the mTOR–ATP binding pocket. These ATP-competitive mTOR agents inhibit both mTORC1 and mTORC2, and have shown preclinically to block tumor cell proliferation more effectively than rapalogs.[5] Because of the highly conserved ATP binding pockets of the PIKK family, the first set of ATP-competitive mTOR molecules proved to be dual PI3K/mTOR inhibitors. A concern for dual PI3K/mTOR inhibitors is the potential effect of insulin resistance and glucose metabolism regulation through the activation of Akt downstream from PI3K.[6] Thus, there have been intense efforts in finding selective mTOR inhibitors that may offer increased tolerability relative to dual PI3K/mTOR inhibitors. Many researchgroups,[7,8] including our own,[9] have reported studies toward identification of selective ATP-competitive mTOR inhibitors.

A high-throughput screen of our corporate compound library identified imidazolopyrimidine **1**[10] as a modestly potent mTOR inhibitor with a K_i of 72 nM (Fig. 1). Introduction of a substituted morpholine at the hinge binding region, and replacement of the aminopyrimidine with a phenyl urea on related pyrimidine scaffolds were reported to increase mTOR potency and selectivity over PI3 kinases.[7] The selectivities were due to the *S*-methyl morpholine packing against a unique Trp2239 residue in mTOR and the ethyl urea interacting hydrophobically with the Cβ and Cγ atoms of the Glu2190 side chain. Thus, the morpholine/aminopyrimdine of **1** was replaced with (*S*)-3-methyl-morpholine/ethyl phenyl urea to provide a more potent and selective mTOR inhibitor **2**. Relative

* Corresponding authors. Tel.: +1 650 225 7704; fax: +1 650 742 4943.
E-mail addresses: wendyle@gene.com (W. Lee), danielfo@gene.com (D.F. Ortwine).

0960-894X/$ - see front matter © 2013 Elsevier Ltd. All rights reserved.
http://dx.doi.org/10.1016/j.bmcl.2013.07.027

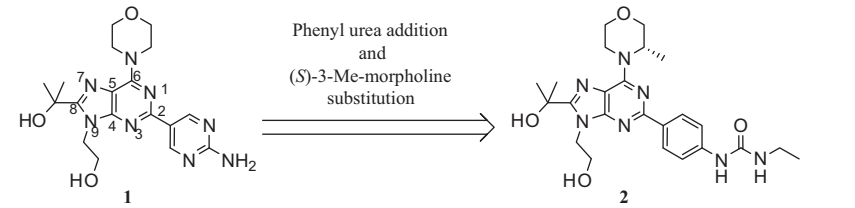

1

mTOR K_i = 72 nM
PI3Kα K_i = 2 nM, PI3Kα / mTOR = 0.03
PI3Kδ K_i = 4 nM, PI3Kδ / mTOR = 0.06

2

mTOR K_i = 9 nM
PI3Kα K_i = 190 nM, PI3Kα / mTOR = 21
PI3Kδ K_i = 160 nM, PI3Kδ / mTOR = 18

Figure 1. Improvement of mTOR potency and selectivities over P13K isoforms.

Table 1
Initial SAR of **2**: mTOR, PI3Kα, and PI3Kδ potencies and selectivities[a,b]

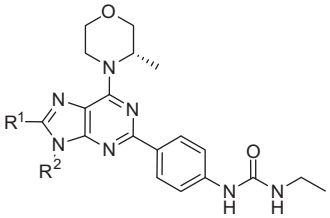

Compd	R^1	R^2	mTOR K_i (nM)	PI3Kα K_i (nM)	PI3Kα/mTOR	PI3Kδ K_i (nM)	PI3Kδ/mTOR
2	$-CH(CH_3)_2OH$	$-CH_2CH_2OH$	9	190	21×	160	18×
3	$-CH(CH_3)_2OH$	Me	7	390	56×	490	70×
4	H	Me	12	370	31×	890	74×

[a] Assays are described in Refs. 9b and 11.
[b] Values are at least two separate determinations with typical variations of less than ±30%.

to **1**, **2** was eightfold more potent (mTOR K_i = 9.5 nM) and exhibited 21- and 17-fold selectivities for mTOR over PI3Kα and PI3Kδ respectively (Fig. 1). Initial SAR exploration by truncation of the 2-hydroxyethyl side chain led to methyl analog **3**, which showed comparable mTOR potency (K_i = 7 nM) with decreased PI3Kα and δ potencies (Table 1). Removal of the *C*-8 tertiary alcohol resulted in **4**, with similar potencies for mTOR (K_i = 12 nM) and PI3Kα (K_i = 370 nM), and a slight decrease in PI3Kδ potency (IC_{50} = 890 nM).

Using a homology model of mTOR built from an X-ray crystal structure of PI3Kγ, we initially hoped to improve selectivity against PI3K by occupying a predicted small hydrophobic pocket adjacent to the morpholine binding region formed by a rigidly held Trp2239 residue (Ile 881 in PI3Kγ). The morpholine oxygenforms a hydrogen bond to the backbone NH of Val2240 in mTOR, in an equivalent location to Val882 in PI3Kγ. Consistent with previous studies,[7a,8e] the (*S*)-3-methyl group on the morpholine of compounds **2**–**4** was predicted to fit into this hydrophobic pocket and pack against Trp2239 without significantly disturbing its conformation (Fig. 2a). An analysis of the morpholine-to-purine bond showed two possible low energy conformations when the ligand was analyzed in vacuo (Supplementary data Fig. S1) However, the same analysis carried out in the presence of the protein showed only one conformer predominated, which placed the (*S*)-3-methyl group adjacent to Tyr2225 (Fig. 2b). Additionally, the morpholino oxygen could adopt an appropriate orientation to engage in an H-bonding interaction with the backbone NH of Val2240 in mTOR.

This proposed binding mode led to a hypothesis in the current work that we may be able to further increase selectivity over PI3K by incorporating a small lipophilic group such as a methyl at the *N*-7 position on the imidazolopyrimidine scaffold. Modeling suggested that this *N*-7-methyl could also pack against the Trp2239 residue, occupying the predicted small hydrophobic pocket in this area. Additionally, the presence of this methyl was predicted to restrict the allowed conformations of the morpholine ring such that the (*S*)-3-methyl group can swing toward Tyr2225 (Supplementary data Fig. S1b). We hoped this would further increase mTOR potency whilemaintaining selectivity against the PI3Kα and PI3Kδ isoforms, without a substantial increase in molecular weight. In this Letter, we describe the synthesis and biological evaluation of a series of mTOR selective *N*-7 substituted imidazolopyrimidines and expand the SAR to include *N*-Me-pyrrolopyrimidine and *N*-Me-pyrazolopyrimidine scaffolds.

N-7-Substituted imidazolopyrimidines **11a**–**f** (Scheme 1) were prepared by alkylation of 4,6-dichloro-1*H*-benzo[*d*]imidazole with either iodomethane or iodoethane under basic conditions to obtain the desired *N*-7-alkylated 2,6-dichloro-imidazolopyrimidine **7a** or **7b**, respectively, in modest yield after separationfrom the major *N*-9 alkylated products **6a** or **6b**. Displacement of **7** with various morpholine derivatives selectively produced 6-morpholino intermediates **9**, which underwent standard Suzuki coupling with the pinacol ester of *N*-ethyl-*N*′-phenyl urea **10** to give *N*-7-alkylated imidazolopyrimidines **11a**–**f**. Regiochemically controlled synthesis of **7a** was accomplished through treatment of theobromine **8** with phosphoryl chloride in the presence of *N*,*N*-diethylaniline, but the overall yield (10–15%) was not superior to N-alkylation.[12] A high yielding method for regiospecific controlled synthesis of **7a** usingtrimethyloxonium borofluorate with *N*-9-(4-methoxybenzyl)purine in 2,2,2,-trifluoroethanol was later reported.[13] To obtain the *C*-8 tertiary alcohol **13** (Scheme 2), **9a** was lithiated at *C*-8 using lithium diisopropylamide and then quenched with acetone, followed by Suzuki coupling, as described above.

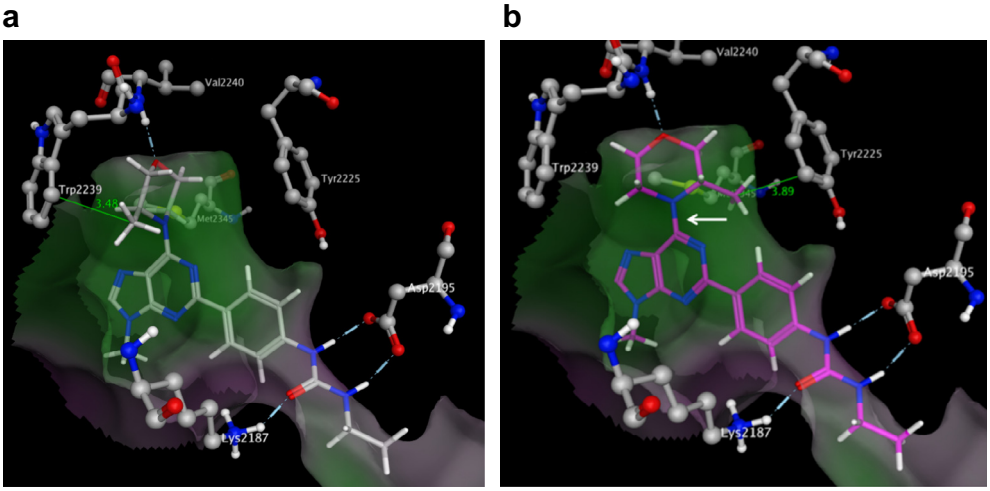

Figure 2. (a) An initial model of **4** docked into a homology model of the mTOR protein. Key residues predicted to contribute to binding and selectivity versus PI3K isoforms are included, as are solvent accessible surfaces color coded by lipophilicity (green = lipophilic, pink = hydrophilic, grey–white = in between). Hydrogen bonds between ligand and protein are shown as hashed lines with cylinders. The distance between the carbon on the (*S*)-3-methyl-morpholine and the closest Trp2239 carbon is shown in green. (b) Model of an alternate conformation of compound **4** docked into a homology model of the mTOR protein. The distance between the carbon on the (*S*)-3-methyl-morpholine and the closest Trp2225 carbon is shown in green.

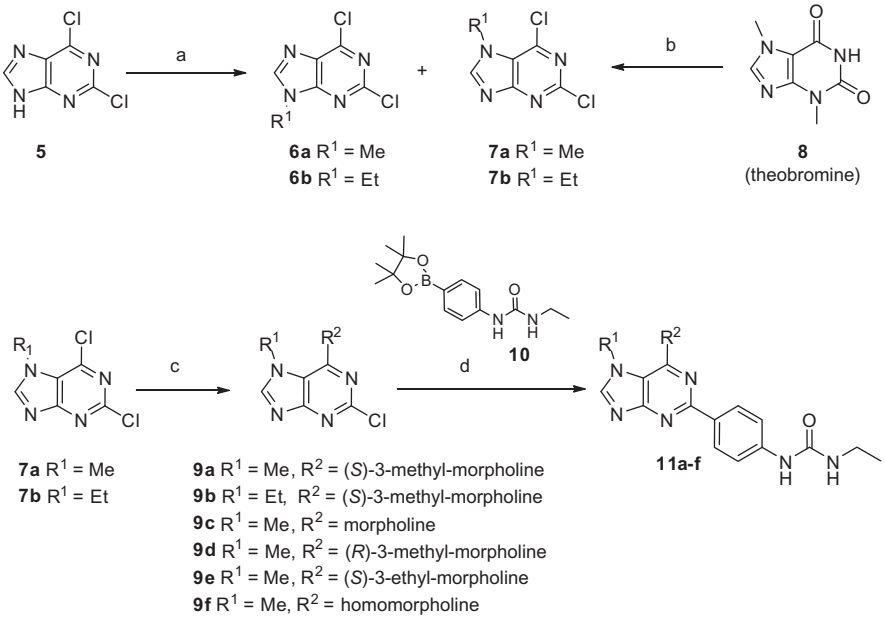

Scheme 1. Reagents and conditions: (a) K_2CO_3, R^1I, acetone, 60 °C, 13% yield; (b) $POCl_3$, *N*,*N*-diethylaniline, 130 °C, 18 h, 10–15% yield; (c) Morpholine derivatives, DIPEA, DMF, 60 °C, 70–85% yield; (d) $(PPh_3)_4Pd$, KOAc, Na_2CO_3, ACN, H_2O, 7–50% yield.

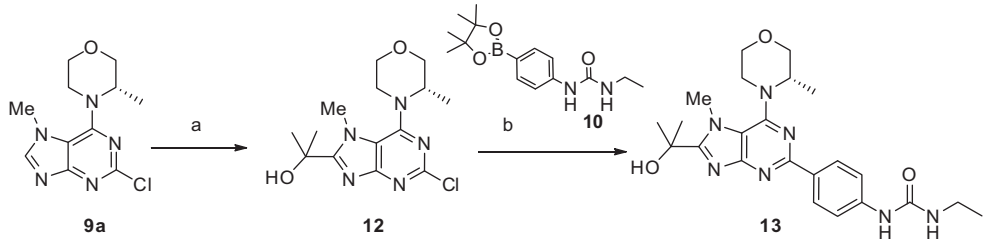

Scheme 2. Reagents and conditions: (a) (i) 5 equiv LDA, THF, −78 °C, 1 h, (ii) excess acetone. −78 °C to rt. Overall 60% yield; (b) $(PPh_3)_4Pd$, KOAc, Na_2CO_3, ACN, H_2O, 45% yield.

Following the same methodology illustrated in Schemes 1 and 2, *N*-9-alkylated imidazolopyrimidines **2**–**4** and **14** were prepared using the major alkylated products, **6a** and **6b**, as starting intermediates. The *N*-5-methyl-pyrrolo[3,2-*d*]pyrimidinyl analogs **15**–**16**

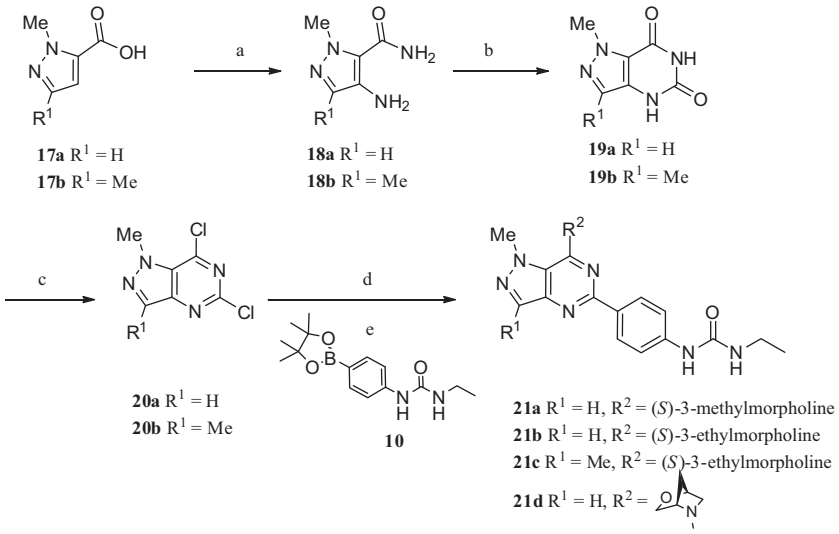

Scheme 3. Reagents and conditions: (a) (i) fuming HNO_3, H_2SO_4, 0 °C, (ii) $SOCl_2$, NH_4OH, 0°C to rt, (iii) 10% Pd/C, EtOH, 60 psi H_2. Overall 46–51% yield; (b) CDI, ACN, reflux 98% yield; (c) $POCl_3$, *N*,*N*-diethylaniline (3:2 v/v), 130 °C. 60–72% yield; (d) morpholine derivatives, DIPEA, DMF, 60 °C. 86–93% yield; (e) $(PPh_3)_4Pd$, KOAc, Na_2CO_3, ACN, H_2O, 54–78% yield.

Table 2
mTOR potency and PI3Kα and PI3Kγ selectivities of *N*-7-Me versus *N*-9-Me-imidazolopyrimidines[a,b]

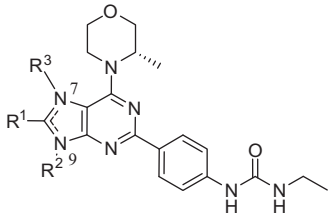

Compd	R^1	(*N*-9) R^2	(*N*-7) R^3	mTOR (nM)	PI3Kα (nM)	PI3Kα/mTOR	PI3Kδ (nM)	PI3Kδ/mTOR
3	$CH(CH_3)_2OH$	Me		7	390	55×	490	68×
13	$CH(CH_3)_2OH$		Me	30	7000	230×	7300	240×
4	H	Me		12	370	30×	890	72×
11a	H		Me	30	>10,000	>330×	>10,000	>330×
14	H	Et		8	380	46×	630	78×
11b	H		Et	40	>10,000	>250×	>10,000	>250×

[a] Assays are described in Refs. 9b and 11.
[b] Values are at least two separate determinations with typical variations of less than ±30%.

were prepared from readily available 2,4-dichloro-5*H*-pyrrolo[3,2-*d*]pyrimidine according to the synthetic route described in Scheme 1.

In order to prepare pyrazolo[4,3-*d*]pyrimidine analogs of **21a–d**, we condensed pyrazolo intermediates **18** with CDI to give pyrimidinediones **19**, which were treated with phosphoryl chloride in the presence of *N*,*N*-diethylaniline to provide dichloropyrimidines **20** (Scheme 3). The pyrazolo intermediates **18a** and **18b** wereprepared following a literature method from readily available 1-methyl-1*H*-pyrazole-5-carboxylic acid and 1,3-dimethyl-1*H*-pyrazole-5-carboxylic acid, respectively.[14] A typical SNAr reaction of **20** with morpholine derivatives followed by Suzuki coupling with the pinacol ester of *N*-ethyl-*N*′-phenyl urea **10** led to the desired *N*-1-methyl-pyrazolo[4,3-*d*]pyrimidines.

All final compounds were tested for inhibition of mTOR, PI3Kα, and PI3Kδ kinases. In vitro mTOR potency was measured with a LanthaScreen FRET assay against recombinant mTOR kinase domain; in vitro PI3K potency was determined using a fluorescence polarization assay against PI3Kα and PI3Kδ as previously described.[9b,11] Cellular potency was measured by the inhibition of phosphorylation of two substrates of mTOR, Akt (serine 473) and p70S6K, in a PTEN-null prostate carcinoma NCI-PC3 cell line. Antiproliferative activity was determined in a 3-day viability assay using NCI-PC3 and MCF7 neo/HER2 cell lines.[11]

A comparison of a small set of *N*-7 versus *N*-9 alkylated imidazolopyrimidines is shown in Table 2. *N*-7 alkylated compounds **13**, **11a**, and **11b** displayed a modest 2.5- to 5-fold decrease in mTOR potency relative to their *N*-9 alkylated counterparts **3**, **4**, and **14**, respectively. The hoped-for increase in mTOR potency of **11a** by the presence of the *N*-7-imidazolopyrimidine methyl group forcing the morpholine (*S*)-3-methyl toward Tyr2225 was not realized (Supplementary data Fig. S1b). However, exquisite selectivities toward the PI3Kα and PI3Kδ isoforms were maintained. The *N*-7-imidazolopyrimidine methyl group may have altered the allowed torsions of the bond connecting the morpholine to the imidazolopyrimidine, subtly affecting the ability of the morpholine oxygen

Table 3
Effect of morpholine derivatives with *N*-7-methyl-imidazopyrimidine[a,b]

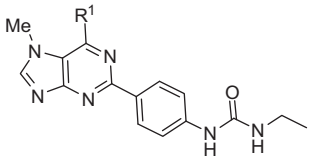

Compd	R^1	Potency/selectivity			Target modulation[c]		Proliferation	
		mTor (K_i nM)	PI3Kα (IC_{50} nM) (fold)	PI3Kδ (IC_{50} nM) (fold)	p-Akt IC_{50}(nM)	Pp70S6K IC_{50} (nM)	NCI-PC3 EC_{50} (nM)	MCF7neo/Her2MDA EC_{50} (nM)
11a		30	>10,000 (>330×)	>10,000 (>330×)	630	2200	290	1300
11c		150						
11d		69	5800 (84×)	4000 (58×)	650	730		
11e	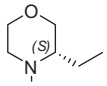	4	>10,000 (>2600×)	>10,000 (>2600×)	69	153	737	518
11f	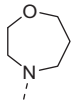	120	6400 (53×)	7300 (61×)	7200	8900		

[a] Assays are described in Refs. 9b and 11.
[b] Values are at least two separate determinations with typical variations of less than ±30%.
[c] Assayed in NCI-PC3 cell line.

to form an optimal hydrogen bond to the backbone NH of Val2240 of mTOR. The modest 2.5- to 5-fold drop in potency for these compounds were difficult to explain with a homology model. The tertiary alcohol at *C*-8 of **11a** was equipotent to *N*-9-Me analog **13** and had no effect on mTOR potency. Modeling predicted that these moieties on *C*-*8* were largely solvent exposed. For **11a** and **11b**, a dramatic reduction in PI3Kα and PI3Kγ potencies was observed, with IC_{50}> 10,000 nM for both isoforms. This was consistent with the hypothesis from modeling that an additive effect between a small lipophilic group at the *N*-7 position on the imidazolopyrimidine and a (*S*)-3-methyl on the morpholine could result in a selectivity gain towards PI3 kinases. The *N*-7 methyl has packed tightly against the face of Trp2239 in mTOR, whereas a non-optimal interaction with the edge of Trp812 (PI3K numbering) was seen in the corresponding region in PI3K. Due to its favorable lead-like properties (clog*P* = 2.2, TPSA = 97, ligand efficiency 0.36), we focused on **11a** as a starting point for evaluating the effects of morpholine substitution.

The mTOR potencies and PI3K selectivities among *N*-7 methyl-imidazolopyrimidine and substituted morpholine analogs are shown in Table 3. Compound **11c**, lacking a methyl group at the 3-position of the morpholine, was five fold less potent against mTOR than **11a**. As mentioned previously, the imidazolopyrimidine *N*-7 methyl may have projected the morpholine 3-methyl group into a space adjacent to Tyr2225 in the homology model (Fig. 2b), partly filling a hydrophobic cavity in the area. Without a 3-methyl substituent occupying the lipophilic pocket created by Tyr2225, the unsubstituted morpholine in **11c** could freely twist to adopt other low energy conformations, effectively increasing the entropy of the system and reducing the potency. The (*R*)-3-methyl enantiomer **11d** showed a two fold drop in mTOR potency relative to the *S*-enantiomer **11a**. To accommodate the morpholine (*R*)-3-methyl into the lipophilic pocket created by Tyr2225, the morpholine may have twisted slightly out-of-plane, altering the optimal hydrogen bond vector from the ring oxygen to the backbone NH of Val2240 of mTOR. Homomorpholine **11f** showed more than a four fold decrease in mTOR activity. An increase in steric clash between the larger homomorpholine and the *N*-7-methyl may have resulted in the homomorpholine ring adopting an out-of-plane conformation, which would be less tolerated by mTOR. Introduction of an (*S*)-3-ethyl substituent on the morpholine (**11e**) resulted in a 7.5-fold gain in mTOR inhibition relative to the (*S*)-3-methyl analog **11a**, leading to a single digit nanomolar inhibitor against mTOR (K_i = 4 nM) while keeping the IC_{50}> 10,000 nM for both PI3K isoforms. *N*-7-methyl substitution restricted the morpholine-to-imidazolopyrimidine torsion angle such that the (*S*)-3-ethyl moiety could fully pack into the hydrophobic space adjacent to Tyr2225 (Fig. 3). Compound **11e** also showed greater than a nine fold potency boost over **11a** in the cellular p-AKT (IC_{50} = 69 nM) and p-p70S6K (IC_{50} = 153 nM) assays, and acceptable anti-proliferative potency in the submicromolar range.

We then extended our *N*-7-alkylated imidazolopyrimidine hypothesis by replacing the heterocyclic core with either pyrrolo[3,2-*d*]pyrimidine or pyrazolo[4,3-*d*]pyrimidine (Table 4). These similar ring systems have been reported as potent PI3K and/or mTOR inhibitors.[8,16] Additionally, the pyrazolo ring nitrogen off the pyrazolopyrimidine can orient more toward solvent and may decrease a desolvation penalty on binding. In the

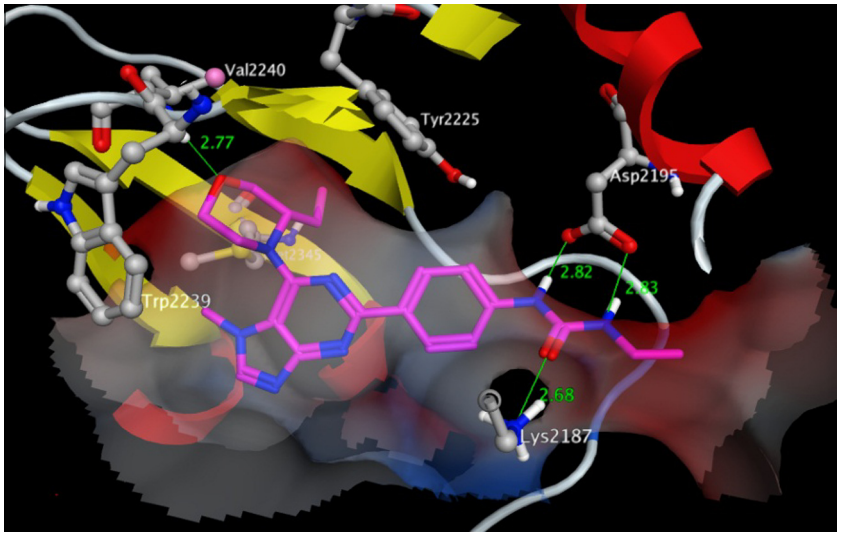

Figure 3. Compound **11e** docked into a homology model of mTOR. Predicted ligand–protein H-bonds are shown in green, with distances between heavy atoms included. A solvent accessible surface of the active site is present, color coded by molecular electrostatic potential calculated using the protein active site atoms (red = negative; blue = positive; white = neutral).[15] Key residues hypothesized to contribute to mTOR potency and selectivity against PI3K isoforms have been included.

Table 4
mTOR, PI3Kα, and PI3Kδ potencies and selectivitites of *N*-methyl-pyrrolo[3,2-*d*]pyrimidines and *N*-methyl-pyrazolo[4,3-*d*]pyrimimdines[a,b]

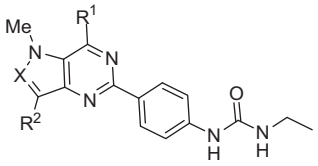

Compd	R^1	R^2	X	Potency/selectivity			Target modulation[c]		Proliferation	
				mTor(K_i nM)	PI3Ka (K_i nM) (fold)	PI3Kd (K_i nM) (fold)	p-Akt IC_{50} (nM)	p-p70S6K IC_{50}(nM)	NCI-PC3 EC_{50} (nM)	MCF7neo/Her2MDA EC_{50} (nM)
15		H	CH	19	>10,000 (>518×)	>10,000 (>518×)	77	110	1900	9000
16	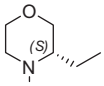	H	CH	6	>10,000 (>1800×)	>10,000 (>1800×)	11	40	280	420
21a		H	N	8	>10,000 (>1290×)	>10,000 (>1290×)	8	47	420	760
21b	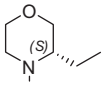	H	N	1	3400 (>2800×)	>10,000 (>8300×)	8	15	130	260
21c	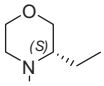	**Me**	**N**	**2**	**5800 (2900×)**	**>10,000 (>5300)**	**4**	**8**	**86**	**160**
21d		H	N	28	5135 (180 ×)	5147 (180x)	340	270	2900	1700

[a] Assays are described in Refs. 9b and 11.
[b] Values are at least two separate determinations with typical variations of less than ±30%.
[c] Assayed in NCI-PC3 cell line.

pyrrolo[3,2-*d*]pyrimidine series, (*S*)-3-Me morpholine **15** and(*S*)-3-Et morpholine **16** had comparable biochemical potency to **11a** and **11e**, respectively. The pyrazolo[4,3-*d*]pyrimidine series displayed increased mTOR inhibition, with **21a** and **21b** displaying single digit nanomolar potency in the mTOR biochemical assay and desirable selectivity against the PI3Kα (>2800×) and PI3Kδ

(>8300×) isoforms. We then explored the SAR of pyrazolo[4,3-*d*]pyrimidines by preparing a bridged morpholine **21d** (*S*,*S* isomer) to evaluate the effect of a constrained morpholine packing against the face of Tyr2225. An *N*-7-methyl substituent with a bridged morpholine was tolerated (K_i = 28 nM) although mTOR potency was reduced 3.7- and23-fold relative to **21a** and **21b**, respectively. This reduction may be due a less tight packing of the extra methylene unit against Tyr2225. This bridged substitution was also reported in a potent morpholine derivative when combined with *N*-9 alkylated pyrazolopyrimidines.[7a] Substitution of *C*-3 on the pyrazolo[4,3-*d*]pyrimidine was also probed. The *C*-3 methyl analog **21c** was equipotent to **21b** and displayed a 2900-fold selectivity toward PI3K. Furthermore, **21c** showed exceptional cellular potencies in single digit nanomolar range [p-AKT IC_{50} = 4 nM and p-p70S6K IC_{50} 8 8 nM] and good anti-proliferative potencies [NCI-PC3EC_{50} = 86 nM and MCF7neo/Her2MDA EC_{50} = 160 nM].

A representative compound (**21a**) from the *N*-Me pyrazolo[4,3-*d*]pyrimidine series was selected for a mouse pharmacokinetic study. The mouse iv profile showed **21a** possessed acceptably low plasma clearance and a low volume of distribution (Cl = 13 mL/min/kg, Vss = 0.36 L/kg). After a 25 mg/kg oral dose, **21a** was found to suffer from non-optimal bioavailability (%*F* = 4.4; dosed orally as a suspension in MCT). The cause for low bioavailability was not permeability or transporter mediated efflux,since a MDCK (Madin–Darby canine kidney epithelial cells) cellular assay of **21a** showed good permeability with minimal efflux potential (Papp B–A = 8.6 $\times 10^{-6}$ cm/s; net flux ratio = 0.55). Limitation of oral absorption may be due to low aqueous solubility, given that the thermodynamic aqueous solubility of **21a** was moderate at 63.2 μM (pH 7.4). Solubility-related physicochemical factors[17] such as compound dissolution in biorelevant media, basicity (pKa), or particle size may also be contributing to its low bioavailability. Compound **21a** was observed to have a partial crystalline form, affecting its solubility due to different dissolution rates and particle sizes (data notshown).

In conclusion, guided by structure-based design, we were able to synthesize and evaluate a variety of *N*-7-Me-imidazolopyrimidines, *N*-5-Me-pyrrolo[3,2-*d*]pyrimidines, and *N*-1-Me-pyrazolo[4,3-*d*]pyrimidines for mTOR inhibition and selectivity against PI3K. We identified *N*-1-Me-pyrazolo[4,3-*d*]pyrimidine as a lead series with exquisite mTOR potency, high selectivity versus PI3Kα and PI3Kδ, and excellent cellular potency. Unfortunately, poor oral bioavailability precluded further development of this series. Subsequent to this work, Xray crystal structures of the mTOR kinase domain have been reported.[18] Our homology model of the protein matched up quite well to the observed residue positions in the active site, validating the useof the model in our structure-based design studies (Supplementary data Fig. S2).

Acknowledgments

The authors gratefully thank the purification and analytical groups within Genentech Small Molecule Drug Discovery for their support. We also thank Dr. James Crawford for helpful discussions and critical review of the manuscript.

Supplementary data

Supplementary data associated with this article can be found, in the online version, at http://dx.doi.org/10.1016/j.bmcl.2013.07.027.

References and notes

1. Laplante, M.; Sabatini, D. M. *Cell* **2012**, *149*, 274.
2. Liu, Q.; Thoreen, C.; Wang, J.; Sabatini, D.; Gray, N. S. *Drug Discovery Today: Ther. Strategies* **2009**, *6*, 47.
3. O'Reilly, K. E.; Rojo, F.; She, Q. B.; Solit, B.; Mills, G. B.; Smith, D.; Lane, H.; Hofmann, F.; Hicklin, D. J.; Ludwig, D. L.; Baselga, J. B.; Rosen, N. *Cancer Res.* **2006**, *66*, 1500.
4. Guertin, D. A.; Sabatini, D. M. *Sci. Signaling* **2009**, *2*, pe 24.
5. Fasolo, A.; Sessa, C. *Expert Opin. Invest. Drugs* **2011**, *20*, 381.
6. (a) Foukas, L. C.; Claret, M.; Pearce, W.; Okkenhaug, K.; Meek, S.; Peskett, E.; Sancho, S.; Smith, A. J. H.; Withers, D. J.; Vanhaesebroeck, B. *Nature* **2006**, *441*, 366; (b) Knight, Z. A.; Gonzalez, B.; Feldman, M. E.; Zunder, E. R.; Goldenberg, D. D.; Williams, O.; Loewith, R.; Stokoe, D.; Balla, A.; Toth, B.; Balla, T.; Weiss, W. A.; Williams, R. L.; Shokat, K. M. A. *Cell* **2006**, *125*, 733.
7. (a) Zask, A.; Kaplan, J.; Verheijen, J. C.; Richard, D. J.; Curran, K.; Brooijmans, N.; Bennett, E. M.; Toral-Barza, L.; Hollander, I.; Ayral-Kaloustian, S.; Yu, K. *J.Med. Chem.* **2009**, *52*, 7942; (b) Nowak, P.; Cole, D. C.; Brooijmans, N.; Bursavich, M. G.; Curran, K. J.; Ellingboe, J. W.; Gibbons, J. J.; Hollander, I.; Hu, Y.; Kaplan, J.; Malwitz, D. J.; Toral-Barza, L.; Verheijen, J. C.; Zask, A.; Zhang, W.-G.; Yu, K. *J.Med. Chem.* **2009**, *52*, 7081; (c) Zask, A.; Verheijen, J. C.; Curran, K.; Kaplan, J.; Richard, J. L.; Nowak, P.; Malwitz, D. J.; Brooijmans, N.; Bard, J.; Svenson, K.; Lucas, J.; Toral-Barza, L.; Zhang, W.-G.; Hollander, I.; Gibbons, J. J.; Abraham, R. T.; Ayral-Kaloustian, S.; Mansour, T. S.; Yu, K. *J.Med. Chem.* **2009**, *52*, 5013; (d) Verheijen, J. C.; Yu, K.; Toral-Barza, L.; Hollander, I.; Zask, A. *Bioorg. Med. Chem.Lett.* **2010**, *20*, 375; (e) Verheijen, J. C.; Richard, D. J.; Curran, K.; Kaplan, J.; Lefever, M.; Nowak, P.; Malwitz, D. J.; Brooijmans, N.; Toral-Barza, L.; Zhang, W.-G.; Lucas, J.; Hollander, I.; Ayral-Kaloustian, S.; Mansour, T. S.; Yu, K.; Zask, A. *J.Med. Chem.* **2009**, *52*, 8010; (f) Curran, K. J.; Verheijen, J. C.; Kaplan, J.; Richard, D. J.; Toral-Barzab, L.; Hollander, I.; Lucas, J.; Ayral-Kaloustiana, S.; Yu, K.; Zask, A. *Bioorg.Med. Chem. Lett.* **2010**, *20*, 1440.
8. (a) Mortensen, D. S.; Sapienza, J.; Lee, B. G. S.; Perrin-Ninkovic, S. M.; Harris, R.; Shevlin, G.; Parnes, J. S.; Whitefield, B.; Hickman, M.; Khmbatta, G.; Bisonette, R. R.; Peng, S.; Gamez, J. C.; Leistend, J.; Krishna, N.; Fultz, K. E.; Sankar, S. *Bioorg.Med. Chem. Lett.* **2013**, *23*, 1588; (b) Takeuchi, C. S.; Kim, B. G.; Blazey, C. M.; Ma, S.; Johnson, H. W. B.; Anand, N. K.; Arcalas, A.; Bail, T. G.; Bur, C. A.; Cannoy, J.; Epshteyn, A. J.; Lara, K.; Lee, M. S.; Wang, L.; Leah, J. W.; Nuss, J. M.; Aay, N.; Aoyama, R.; Foster, P.; Lee, J.; Lehoux, I.; Munagala, N.; Plonowski, A.; Rajan, S.; Woolfrey, J.; Yamaguchi, K.; Lamb, P.; Miller, N. *J.Med. Chem.* **2013**, *56*, 2218; (c) Liu, K. K. C.; Bailey, S.; Dinh, D. M.; Lam, H.; Li, C.; Wells, P. A.; Yin, M.-J.; Zou, A. *Bioorg. Med. Chem.Lett.* **2012**, *22*, 5114; (d) Peterson, E. A.; Boezio, A. A.; Andrews, P. S.; Boezio, C. M.; Bush, T. L.; Cheng, A. C.; Choquette, D.; Coats, J. R.; Colletti, A. E.; Copeland, K. W.; DuPont, M.; Graceffa, R.; Grubinska, B.; Kim, J. L.; Lewis, R. T.; Liu, J.; Mullady, E.; Potashman, M. H.; Romero, K.; Shaffer, P. L.; Stanton, M. K.; Stellwagen, J. C.; Teffera, Y.; Yi, S.; Cai, T.; La, D. S. *Bioorg.Med. Chem. Lett.* **2012**, *22*, 4967; (e) Finlay, M. R. V.; Buttar, D.; Critchlow, S. E.; Dishington, A. P.; Fillery, S. M.; Fisher, E.; Glossop, S. C.; Graham, M. A.; Johnson, T.; Lamont, G. M.; Mutton, S.; Perkins, P.; Pike, K. G.; Slater, A. M. *Bioorg.Med. Chem. Lett.* **2012**, *22*, 4163; (f) Liu, Q.; Wang, J.; Kang, S. A.; Thoreen, C. C.; Hur, W.; Ahmed, T.; Sabatini, D. M.; Gray, N. S. *J. Med.Chem.* **2011**, *54*, 1473.
9. (a) Estrada, A. A.; Shore, D. J.; Blackwood, E.; Chen, Y.-H.; Deshmukh, G.; Ding, X.; DiPasquale, A. G.; Epler, J. A.; Friedman, L. S.; Koehler, M. F. T.; Liu, L.; Malek, S.; Nonomiya, J.; Ortwine, J. F.; Pei, Z.; Sideris, S.; St-Jean, F.; Trinh, L.; Truong, T.; Lyssikatos, J. P. *J.Med. Chem.* **2013**, *56*, 3090; (b) Pei, Z.; Blackwood, E.; Liu, L.; Malek, S.; Belvin, M.; Koehler, M. F. T.; Ortwine, D. F.; Chen, H.; Cohen, F.; Kenny, J. R.; Bergeron, P.; Lau, K.; Ly, C.; Zhao, X.; Estrada, A. A.; Truong, T.; Epler, J. A.; Nonomiya, J.; Trinh, L.; Sideris, S.; Lesnick, J.; Bao, L.; Vijapurkar, U.; Mukadam, S.; Tay, S.; Deshmukh, G.; Chen, Y. H.; Ding, X.; Friedman, L. S.; Lyssikatos, J. P. *ACSMed. Chem. Lett.* **2013**, *4*, 103; (c) Koehler, M. F. T.; Bergeron, P.; Blackwood, E.; Bowman, K. K.; Chen, Y. H.; Deshmukh, G.; Ding, X.; Epler, J.; Lau, K.; Lee, L.; Liu, L.; Ly, C.; Malek, S.; Nonomiya, J.; Oeh, J.; Ortwine, D. F.; Sampath, D.; Sideris, S.; Trinh, L.; Truong, T.; Wu, J.; Pei, Z.; Lyssikatos, J. P. *J.Med. Chem.* **2012**, *55*, 10958; (d) Cohen, F.; Bergeron, P.; Blackwood, E.; Bowman, K. K.; Chen, Y. H.; DiPasquale, A. G.; Epler, J. A.; Koehler, M. F. T.; Lau, K.; Lewis, C.; Liu, L.; Ly, C. Q.; Malek, S.; Nonomiya, J.; Ortwine, D. F.; Pei, Z.; Robarge, K. D.; Sideris, S.; Trinh, L.; Truong, T.; Wu, J.; Zhao, X.; Lyssikatos, J. P. *J.Med. Chem.* **2011**, *54*, 3426.
10. Compound was disclosed in: Castanedo, G.; Chuckowree, I.; Folkes, A.; Sutherlin, D. P.; Wan, N. C. WO 2009146406, **2009**.
11. Sutherlin, D. P.; Sampath, D.; Berry, M.; Castanedo, G.; Chang, Z.; Chuckowree, I.; Dotson, J.; Folkes, A.; Friedman, L.; Goldsmith, R.; Heffron, T.; Lee, L.; Lesnick, J.; Lewis, C.; Mathieu, S.; Nonomiya, J.; Olivero, A.; Pang, J.; Prior, W.; Salphati, L.; Sideris, S.; Tian, Q.; Tsui, V.; Wan, N. C.; Wang, S.; Wiesmann, C.; Wong, S.; Zhu, B.-Y. *J.Med. Chem.* **2010**, *53*, 1086.
12. Uretskaya, G. Ya.; Rybinka, E. I.; Men'shikov, G. P. *Zh. Obshch. Khim.* **1960**, *30*, 327.
13. Lebraud, H.; Cano, C.; Carbain, B.; Hardcastle, I. R.; Harringon, R. W.; Griffin, R. J.; Golding, B. T. *Org. Biomol.Chem.* **1874**, *2013*, 11.
14. Terrett, N. K.; Bell, A. S.; Brown, D.; Ellis, P. *Bioorg. Med. Chem. Lett.* **1819**, *1996*, 6.
15. The surface is color coded by a screened (localized) electrostatic potential that uses a charge density obtained by solving the Poisson–Boltzmann equation using MMFF94 partial charges on the protein. Default values for the color scale range were used, as provided in the MOE software (www.chemcomp.com).
16. (a) Chen, Z.; Venkatesan, A. M.; Dehnhardt, C. M.; Ayral-Kaloustian, S.; Brooijmans, N.; Mallon, R.; Feldberg, L.; Hollander, I.; Lucas, J.; Yu, K.; Kong, F.; Mansour, T. S. *J.Med. Chem.* **2010**, *53*, 3169; (b) Gilbert, A. M.; Nowak, P.; Brooijmans, N.; Bursavich, M. G.; Dehnhardt, C.; Santos, E. D.; Feldberg, L. R.;

Hollander, I.; Kim, S.; Lombardi, S.; Park, K.; Venkatesan, A. M.; Mallon, R. *Bioorg.Med. Chem. Lett.* **2010**, *20*, 636; (c) Hayakawa, M.; Kaizawa, H.; Moritomo, H.; Kawaguchi, K.; Koizumi, T.; Yamano, M.; Matsuda, K.; Okada, M.; Ohta, M. WO 2001083456, **2001**.; (d) Zask, A.; Verheijen, J. C.; Richard, D. J. *Expert Opin. Ther.Patents* **2011**, *21*, 1109.

17. Thomas, V. H.; Bhattachar, S.; Hitchingham, L.; Zocharski, P.; Naath, M. Surendran, N,; Stoner, C. L., El-Kattan, A *Expert Opin. Drug Metabol. Toxicol.* **2006**, *2*, 591.
18. Yang, H.; Rudge, D. G.; Koos, J. D.; Vaidialingam, B.; Yang, H. J.; Pavletich, N. P. *Nature* **2013**, *497*, 217.